Metal–Semiconductor Nanostructures

DOI: 10.1002/anie.200806082

A General Approach to the Synthesis of Gold–Metal Sulfide Core–Shell and Heterostructures**

*Zhenhua Sun, Zhi Yang, Jianhua Zhou, Man Hau Yeung, Weihai Ni, Hongkai Wu, and Jianfang Wang**

A significant step after the remarkable success in growing single-component nanocrystals is the preparation of nanostructures that are composed with discrete domains of different materials. The attraction of multicomponent nanostructures is that multiple functions can be integrated into one system for specific applications.[1–5] Moreover, the interactions between nanoscale-spaced components can greatly improve the overall application performance of the nanostructured system and even generate new synergetic properties. For example, in noble metal–semiconductor nanostructures, metallic ingredients can improve the charge separation[6–11] and enhance light absorption in semiconductors.[12,13] Both effects can increase the photocatalytic and light-harvesting efficiencies of semiconductors. Metallic ingredients can also alter the luminescence behavior of semiconductors.[14–17] Furthermore, the coupling of semiconductor and noble metal components allows the plasmonic modes of the latter to be excited and controlled for information processing and transmission.[18,19] Herein we report a general method for the synthesis of water-dispersible gold–metal sulfide core–shell and heterostructures. Hybrid nanostructures made up of Au nanocrystals of varying shapes and different transition metal sulfide semiconductors (ZnS, CdS, Ag_2S, NiS, and CuS) have been successfully synthesized following a similar procedure.

Methods previously developed for the synthesis of metal–semiconductor nanostructures include selective growth of metals onto the tips and surfaces of semiconductor nanocrystals,[10,17,20–25] photodeposition of metals on semiconductor nanorods,[26] diffusion of metals into semiconductors,[27] and growth of semiconductors on metal seeds.[13,28–34] These methods often involve growth in organic solvents, and therefore yield nanostructures that are not suitable for photocatalytic cleaning and biological applications. In addition, most of the products obtained from these methods are heterostructures. Only a few examples of metal–semiconductor core–shell nanostructures have been reported to date,[13,28,31,33] although the core–shell geometry can maximize the interfacial area and thus provide a platform for studying the plasmon–exciton interactions and charge distributions. Furthermore, with previous methods, control of the shapes and sizes of noble metal components remains a challenge. This controllability is highly important for studying the plasmon–exciton interactions and even tailoring them for improved application performances, because the plasmonic properties of noble metals are strongly dependent on their shapes and sizes.

The use of pregrown Au nanocrystals for the synthesis of gold–metal sulfide nanostructures allows their shapes and sizes, and thus their plasmonic properties, to be rationally chosen. In our synthesis (Figure 1), Au nanocrystals in polyhedron, cube, and rod shapes were used (see the Supporting Information, Figure S1). The average diameter of Au nanopolyhedra, edge length of Au nanocubes, and diameter/length of Au nanorods used were (43 ± 1), (50 ± 3), and $(14\pm2)/(58\pm6)$ nm, respectively. The ensemble surface plasmon resonance wavelengths (SPRWs) of the nanopolyhedra and nanocubes in aqueous solutions were 535 and 545 nm, respectively. The nanorods had a transverse SPRW at 512 nm and longitudinal SPRW at 846 nm. Their particle concentrations were estimated to be 0.05, 0.02, and 0.9 nM,

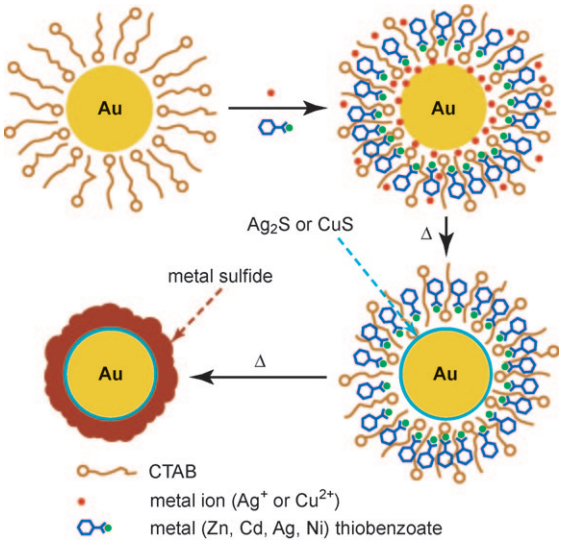

Figure 1. Synthetic method for growth of Au–metal sulfide core–shell structures. Cetyltrimethylammonium bromide (CTAB) enhances the solubility of metal thiobenzoates in aqueous solutions. Ag_2S or CuS acts as a wetting layer to help in the deposition of other metal sulfides on Au nanocrystals.

[*] Dr. Z. H. Sun, Dr. Z. Yang, M. H. Yeung, Dr. W. H. Ni, Prof. J. F. Wang
Department of Physics, The Chinese University of Hong Kong
Shatin, Hong Kong SAR (China)
Fax: (+852) 2603-5204
E-mail: jfwang@phy.cuhk.edu.hk
J. H. Zhou, Prof. H. K. Wu
Department of Chemistry, The Hong Kong University of Science and Technology
Clear Water Bay, Kowloon, Hong Kong SAR (China)

[**] This work was supported by Hong Kong RGC Direct Allocation (Project Code: 2060332) and the Joint Research Scheme between NSFC and Hong Kong RGC (Reference: N_CUHK448/06, Project Code: 2900318).

Supporting information for this article is available on the WWW under http://dx.doi.org/10.1002/anie.200806082.

respectively. These Au nanocrystals were stabilized in aqueous solutions by 0.1M cetyltrimethylammonium bromide (CTAB), which forms a bilayer on their surfaces.[35] Metal thiobenzoates, including Zn, Cd, Ag, and Ni, are insoluble in water, but they can be dissolved in aqueous CTAB solutions. The solubility enhancement is believed to result from the hydrophobic interaction between the tail of CTAB and the benzene ring of the metal complexes. The presence of a small amount of Ag^+ or Cu^{2+} ions, which was supplied in the form of either inorganic salts or metal thiobenzoates, was found to be necessary for the deposition of metal sulfides on Au nanocrystals (see the Supporting Information, Figure S2). Under hydrothermal conditions, metal thiobenzoates decomposed and provided sulfur for Ag^+ or Cu^{2+} ions to form sulfides. The resultant Ag_2S or CuS are bound tightly to Au nanocrystals owing to the similarity in the chemical properties among Cu, Ag, and Au. They act as a wetting layer for the deposition of other metal sulfides that are generated hydrothermally from the corresponding thiobenzoates (see the Supporting Information, Figure S3). The function of Ag_2S or CuS as a wetting layer can be ascribed to the partial cation exchange among different metal sulfides. The cation-exchange reactions among metal chalcogenides have previously been applied to the preparation of various metal chalcogenide nanostructures.[36–38]

Figure 2 shows the scanning electron microscopy (SEM) and transmission electron microscopy (TEM) images of Au nanopolyhedron–ZnS core–shell (nanopolyhedron@ZnS) structures and their structural, elemental, and optical characterizations. With a low concentration of Ag^+ (14.5 μM), the resultant ZnS shells were composed of loosely aggregated ZnS nanoparticles (Figure 2a,b), whereas with a high concentration of Ag^+ (100 μM), dense ZnS shells were obtained (Figure 2c,d). The increase in packing density of the ZnS nanoparticles in the shell resulted from the deposition of more Ag_2S, which functions as a binder between ZnS and the surfaces of Au nanopolyhedra. This dependence of the ZnS shell packing density on the concentration of Ag^+ allowed the SPRW of the resultant core–shell nanostructures to be readily tailored over a wide spectral range. As the concentration of Ag^+ was increased from 14.5 to 200 μM, the core–shell nanostructures exhibited a clear color change and their plasmon resonance peaks red-shifted from 550 to 760 nm, owing to an increase in the refractive index of the medium surrounding the Au nanopolyhedra (Figure 2e).[39,40] The core–shell nanostructures contained only Au, Zn, S, and Ag, as indicated by the energy dispersive X-ray (EDX) spectra (see the Supporting Information, Figure S4). High-angle annular dark-field (HAADF) scanning transmission-electron

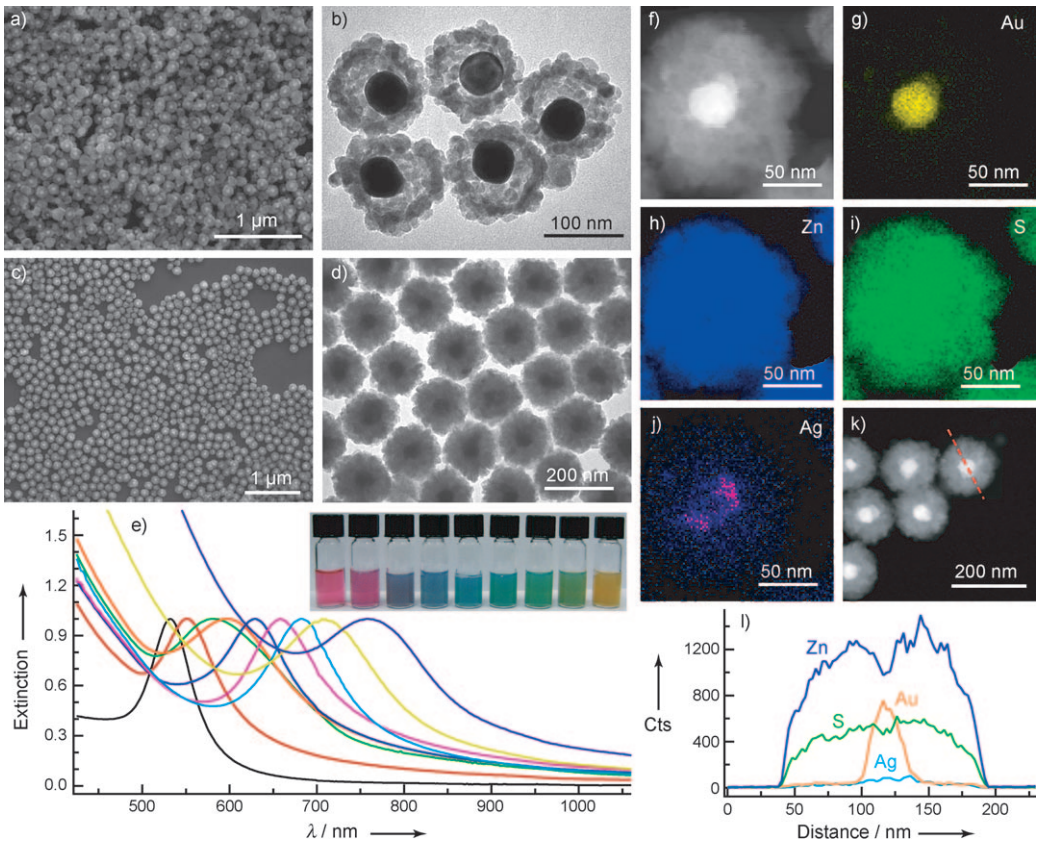

Figure 2. Gold nanopolyhedron@ZnS structures: a) SEM image. b) TEM image. c) SEM image. d) TEM image. The average diameter of the structures shown in (a) and (b) is (125 ± 6) nm, and that in (c) and (d) is (135 ± 8) nm. The concentrations of Ag^+ for the synthesis of the two samples are 14.5 and 100 μM, respectively. e) Normalized extinction spectra and corresponding digital images (inset, from left to right) of core–shell structures synthesized at increasing Ag^+ concentrations. The black curve is the spectrum of the starting Au nanopolyhedra. f) HAADF-STEM image of one core–shell structure. g–j) EDX elemental maps of Au, Zn, S, and Ag, respectively. k) HAADF-STEM image. l) Line profiles of Au, Zn, S, and Ag recorded along the dashed line shown in (k). The concentration of Ag^+ during synthesis for the sample shown in (f–l) is 100 μM, and that of $(PhCOS)_2Zn$ for all the samples shown in (a–l) is 2.4 mM.

microscopy (STEM) imaging, in conjunction with EDX elemental mapping and line profiling (Figure 2 f–l), revealed that the core was composed of Au and the shell was mainly composed of Zn and S. A small amount of Ag was detected in the region surrounding the Au core, confirming the intermediate binding role of Ag_2S between the core and shell. In addition, the ZnS nanoparticles in the shell had a zinc blende crystal structure, as indicated by X-ray diffraction (XRD) and high-resolution TEM (HRTEM) measurements (see the Supporting Information, Figure S5).

Zinc thiobenzoate was also treated under similar hydrothermal conditions in the absence of Ag^+ or Au nanocrystals (see the Supporting Information, Figure S2). Without Ag^+, hollow ZnS spheres were obtained, together with large unencapsulated irregularly shaped Au crystals. In the absence of both Ag^+ and Au nanocrystals, solid ZnS spheres were produced. These results suggest again that Au nanocrystals act as seeds for the growth of ZnS shells and that Ag_2S functions as the intermediate binder between the shell material and Au core. Without the formation of Ag_2S, Au core nanocrystals will be etched, resulting in the production of large Au crystals outside of the shell.

The synthetic method described above was also employed to prepare Au nanocrystal@CdS structures (Figure 3), simply by replacing zinc thiobenzoate with cadmium thiobenzoate. Unlike the nanopolyhedron@ZnS structures, the nanopolyhedron@CdS structures incorporated a dense CdS shell in all cases. Elemental mapping (see the Supporting Information, Figure S6) showed that a considerable amount of Ag was distributed throughout the shell, which suggests that the cation exchange reaction between CdS and Ag_2S is faster than that between ZnS and Ag_2S. Owing to the independence of the shell density on the concentration of Ag^+, the SPRWs of the Au nanopolyhedron@CdS structures increased only slightly from 645 to 670 nm with the increase in concentration of Ag^+ from 40 to 200 μM (Figure 3c). Structural characterization by XRD and HRTEM indicated that the CdS shell had a wurtzite crystal structure (see the Supporting Information, Figure S7).

Silver sulfide readily grows on the surface of Au nanocrystals, so it seemed natural to apply our method to the preparation of Au–Ag_2S core–shell nanostructures (Figure 4). The cores of nanostructures obtained from the synthesis involving Au nanorods (Figure 4a) contained shorter nanorods than the starting material. The shells comprised AgAuS with a cubic crystal structure (see the Supporting Information, Figure S8). The incorporation of Au in the shell is believed to result from the etching of Au nanorods during the hydrothermal process, which is consistent with the reduction in length of the Au nanorods after formation of the core–shell structures. The preparation of nanostructures with Au nanocubes (Figure 4b) and nanopolyhedra (see the Supporting Information, Figure S9) also produced core–shell structures. However, in both of these cases, the shells were composed of Ag_2S with a monoclinic crystal structure. Owing to the increase in Ag_2S shell thickness, the Au nanocube@Ag_2S structures underwent a clear color change compared to the starting nanotubes. The SPRW increased from 635 to 765 nm as the concentration of Ag^+ was increased from 40 to 200 μM (Figure 4c). The formation of different shell structures can be

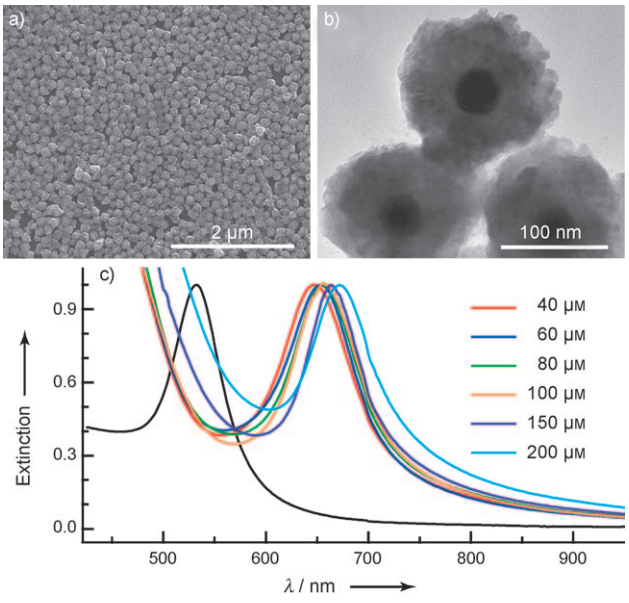

Figure 3. Gold nanopolyhedron@CdS structures: a) SEM image. b) TEM image. The average diameter of the structures shown in (a) and (b) is (139 ± 11) nm. c) Normalized extinction spectra of core–shell structures synthesized at increasing Ag^+ concentrations. The black curve is the spectrum of the starting Au nanopolyhedra. The concentration of $(PhCOS)_2Cd$ during synthesis for all the samples shown in (a–c) is 2.1 mM.

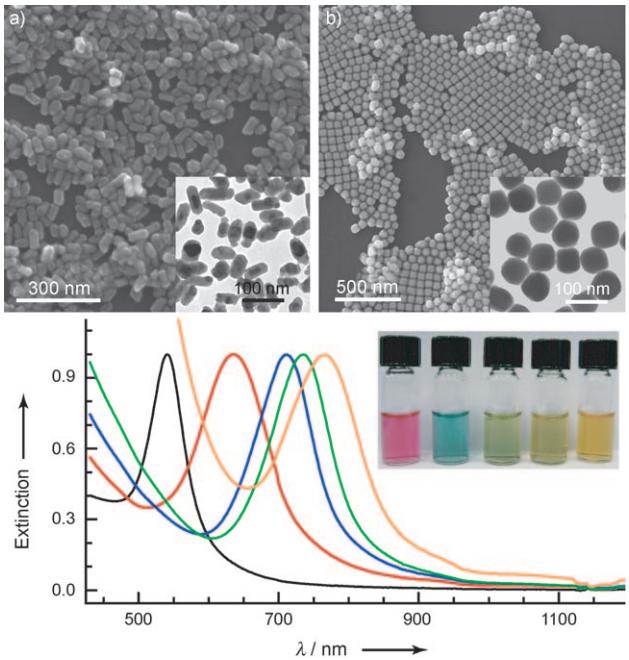

Figure 4. Core–shell structures synthesized from Au nanocrystals and PhCOSAg: a) SEM and TEM (inset) image of Au nanorod@AgAuS structures. b) SEM and TEM (inset) image of Au nanocube@Ag_2S structures. The concentrations of PhCOSAg during synthesis for the samples shown in (a) and (b) are 300 and 100 μM, respectively. c) Normalized extinction spectra and corresponding digital images (inset, from left to right) of Au nanocube@Ag_2S structures synthesized at increasing PhCOSAg concentrations. The black curve is the spectrum of the starting Au nanocubes.

ascribed to the stability difference of the Au nanocrystals with different shapes. The Au nanorods, having highly curved ends owing to their smaller diameters, are less stable towards etching than the Au nanocubes and nanopolyhedra under hydrothermal conditions.[41,42]

The successful preparation of Au nanocrystal–metal sulfide nanostructures required the presence of a wetting layer with the targeted metal sulfides. Although Ag_2S assisted in the deposition of zinc and cadmium sulfides, it was found to be unsuitable for the deposition of nickel sulfide. Instead, a CuS wetting layer was required. Stable copper(II) thiobenzoate cannot be synthesized, so $Cu(NO_3)_2$ was used in our preparation. The resultant structures were composed of dense nickel sulfide shells surrounding core Au nanocrystals (Figure 5a,b). Nickel sulfide is known to possess many polymorphs and stoichiometries. The shell obtained in our preparation was tentatively assigned to be NiS_2 with a cubic crystal structure according to HRTEM imaging (see the Supporting Information, Figure S10). In addition to nickel sulfide, CuS can also mediate the formation of Au nanocrystal@zinc sulfide structures.

As a final demonstration of the generality and flexibility of our synthetic method, we prepared Au nanocrystal–copper sulfide core–shell nanostructures and heterostructures. Since stable copper thiobenzoate is not available, sulfur was supplied by adding nickel thiobenzoate to the reaction solution. The deposition of copper sulfide on the Au nanocrystals, instead of nickel sulfide, was realized by increasing the molar ratio of Cu^{2+} to Ni^{2+}, because copper sulfide grows preferentially on the Au surface under hydrothermal conditions. During the CuS-assisted formation of nickel sulfide shells, the concentration of Cu^{2+} was 80 μM and the molar ratio of Cu^{2+} to Ni^{2+} was 1:30. When the molar ratio of Cu^{2+} to Ni^{2+} was increased to 1:6, the synthesis with Au nanocubes gave core–shell structures (Figure 5c). The shell was composed of hexagonal crystalline CuS with small protruding flakes (see the Supporting Information, Figure S11). No Ni was detected by EDX. When the molar ratio of Cu^{2+} to Ni^{2+} was increased to 1:2, the CuS flakes on the core–shell structures grew larger and also formed stems (Figure 5d). The stems were characterized as cubic crystalline Cu_2S with a deficiency of Cu (see the Supporting Information, Figure S11). The formation of Cu-deficient Cu_2S, instead of CuS, was due to the increase in molar ratio of Cu to S in the reaction solution. Similar core–shell structures were also obtained with Au nanopolyhedra. When Au nanorods were utilized, copper sulfide was preferentially deposited on one side of each Au nanorod, thus forming Au nanorod–copper sulfide heterostructures (Figure 5e,f). These results indicate that the growth behavior of copper sulfide on Au nanorods is different from that of silver sulfide.

In summary, we have developed a facile and general strategy for the synthesis of water-dispersible gold–transition metal sulfide core–shell and heterostructures. The synthesis employs CTAB-encapsulated Au nanocrystals as starting reactants and metal thiobenzoates as metal sulfide precursors. The formation of metal sulfide shells on Au nanocrystals was facilitated both by the presence of CTAB, which helps in dissolving metal thiobenzoates, and by the formation of a

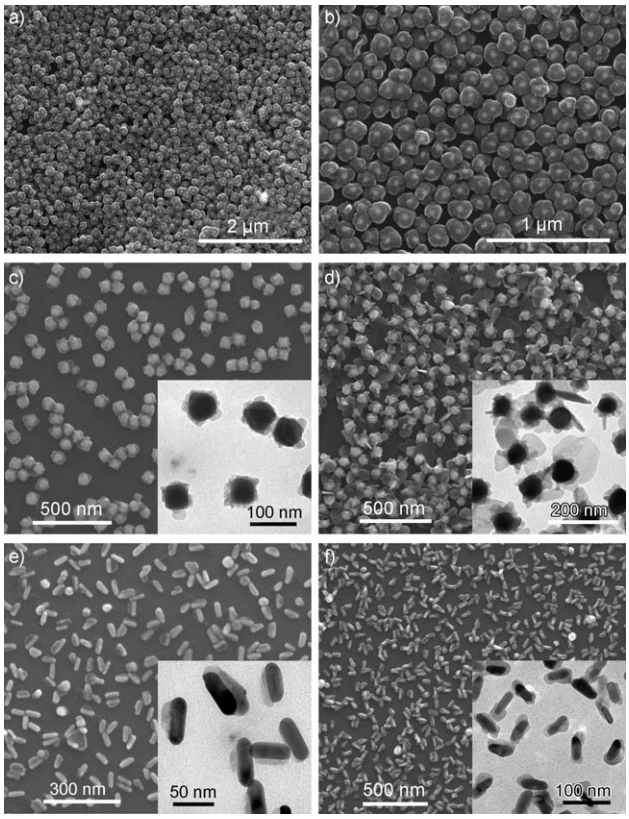

Figure 5. Core–shell and heterostructures involving nickel sulfide and copper sulfide: a) Low-magnification SEM image of Au nanopolyhedron@$Ni_{1-x}S$ structures. b) High-magnification SEM image of the sample shown in (a). The concentrations of $Cu(NO_3)_2$ and $(PhCOS)_2Ni$ during synthesis for the sample shown in (a) and (b) are 80 μM and 2.4 mM, respectively. c) SEM and TEM (inset) image of Au nanocube@CuS structures. The concentrations of $Cu(NO_3)_2$ and $(PhCOS)_2Ni$ during synthesis are 100 and 600 μM, respectively. d) SEM and TEM (inset) image of Au nanocube@$Cu_{2-x}S$ structures. The concentrations of $Cu(NO_3)_2$ and $(PhCOS)_2Ni$ during synthesis are 300 and 600 μM, respectively. e) SEM and TEM (inset) image of Au nanorod-$Cu_{2-x}S$ heterostructures. The concentrations of $Cu(NO_3)_2$ and $(PhCOS)_2Ni$ during synthesis are 100 and 600 μM, respectively. f) SEM and TEM (inset) image of Au nanorod-$Cu_{2-x}S$ heterostructures. The concentrations of $Cu(NO_3)_2$ and $(PhCOS)_2Ni$ during synthesis are 300 and 600 μM, respectively.

Ag_2S or CuS wetting layer. With this strategy, core–shell and/or heterostructures, incorporating differently shaped Au nanocrystals and various metal sulfide semiconductors (ZnS, CdS, Ag_2S, NiS, and CuS), have been successfully produced. We believe that our synthetic strategy can be readily extended to the preparation of core–shell and heterostructures of Au nanocrystals with metal selenide and telluride semiconductors. Such core–shell and heterostructures of gold and transition metal chalcogenide semiconductors will find many applications in photocatalysis, photovoltaics, plasmonics, and optics.

Experimental Section

Gold nanocrystals were prepared using a seeded growth method. Specifically, Au nanorods were grown according to our previously

described procedure[42] (see the Supporting Information for details). Au nanocubes[43,44] and nanopolyhedra[45] were both synthesized according to the reported procedures.

Metal thiobenzoates were obtained as precipitates from the reactions between sodium thiobenzoate and metal chlorides or nitrates in aqueous solutions, as described previously.[46]

Gold–metal sulfide hybrid nanostructures were prepared by mixing together appropriate amounts of Au nanocrystals, metal thiobenzoates, and Ag^+/Cu^{2+} ions in aqueous CTAB solutions and subsequently carrying out a hydrothermal treatment. In a typical preparation, an as-prepared aqueous Au nanocrystal dispersion (10 mL; the concentrations vary for differently-shaped Au nanocrystals. They are given in the main text) was precipitated by centrifugation and then redispersed in 0.1M aqueous CTAB solution (10 mL). A calculated amount of metal thiobenzoate (0.0005–0.03 mmol) was dissolved in this solution, followed by the addition of 0.01M aqueous $AgNO_3$ or $Cu(NO_3)_2$ solution to give controlled concentrations of Ag^+ and Cu^{2+} of 10–200 μM and 80–300 μM, respectively. The resultant mixture was transferred to a Teflon-lined 25 mL autoclave and heated at 140°C for 3 h. The solid products were collected by centrifugation, washed with water (2×10 mL), and redispersed in water for further characterization.

Extinction spectra were measured on a Hitachi U-3501 UV/Vis/NIR spectrophotometer. XRD data were collected using a Bruker D8 Advance diffractometer with $Cu_{K\alpha}$ radiation. Low-magnification TEM imaging was performed on a FEI CM120 microscope. HRTEM, and HAADF-STEM characterizations were carried out on a FEI Tecnai F20 microscope equipped with an Oxford EDX analysis system. SEM images were acquired using a FEI Quanta 400 FEG microscope equipped with an Oxford EDX analysis system. Samples were deposited on Si substrates for XRD and SEM characterizations, and on carbon film-coated copper grids for TEM characterization. Digital pictures were taken using a Canon IXUS 65 camera with an exposure time of 1/16 s.

Received: December 13, 2008
Revised: January 18, 2009
Published online: March 13, 2009

Keywords: gold · metal sulfides · nanostructures · semiconductors · surface plasmon resonance

[1] J. Lee, J. Yang, H. Ko, S. Oh, J. Kang, J. Son, K. Lee, S.-W. Lee, H.-G. Yoon, J.-S. Suh, Y.-M. Huh, S. Haam, *Adv. Funct. Mater.* **2008**, *18*, 258.
[2] J. Kim, J. E. Lee, S. H. Lee, J. H. Yu, J. H. Lee, T. G. Park, T. Hyeon, *Adv. Mater.* **2008**, *20*, 478.
[3] L. Y. Wang, J. W. Bai, Y. J. Li, Y. Huang, *Angew. Chem.* **2008**, *120*, 2473; *Angew. Chem. Int. Ed.* **2008**, *47*, 2439.
[4] J. Kim, H. S. Kim, N. Lee, T. Kim, H. Kim, T. Yu, I. C. Song, W. K. Moon, T. Hyeon, *Angew. Chem.* **2008**, *120*, 8566; *Angew. Chem. Int. Ed.* **2008**, *47*, 8438.
[5] J. H. Gao, G. L. Liang, J. S. Cheung, Y. Pan, Y. Kuang, F. Zhao, B. Zhang, X. X. Zhang, E. X. Wu, B. Xu, *J. Am. Chem. Soc.* **2008**, *130*, 11828.
[6] M. Jakob, H. Levanon, P. V. Kamat, *Nano Lett.* **2003**, *3*, 353.
[7] V. Subramanian, E. E. Wolf, P. V. Kamat, *J. Am. Chem. Soc.* **2004**, *126*, 4943.
[8] Y. Tian, T. Tatsuma, *J. Am. Chem. Soc.* **2005**, *127*, 7632.
[9] H. Tada, T. Mitsui, T. Kiyonaga, T. Akita, K. Tanaka, *Nat. Mater.* **2006**, *5*, 782.
[10] R. Costi, A. E. Saunders, E. Elmalem, A. Salant, U. Banin, *Nano Lett.* **2008**, *8*, 637.
[11] E. Formo, E. Lee, D. Campbell, Y. N. Xia, *Nano Lett.* **2008**, *8*, 668.
[12] K. Awazu, M. Fujimaki, C. Rockstuhl, J. Tominaga, H. Murakami, Y. Ohki, N. Yoshida, T. Watanabe, *J. Am. Chem. Soc.* **2008**, *130*, 1676.
[13] J.-S. Lee, E. V. Shevchenko, D. V. Talapin, *J. Am. Chem. Soc.* **2008**, *130*, 9673.
[14] K. Okamoto, I. Niki, A. Shvartser, Y. Narukawa, T. Mukai, A. Scherer, *Nat. Mater.* **2004**, *3*, 601.
[15] N. G. Liu, B. S. Prall, V. I. Klimov, *J. Am. Chem. Soc.* **2006**, *128*, 15362.
[16] P. P. Pompa, L. Martiradonna, A. D. Torre, F. D. Sala, L. Manna, M. de Vittorio, F. Calabi, R. Cingolani, R. Rinaldi, *Nat. Nanotechnol.* **2006**, *1*, 126.
[17] T. Mokari, E. Rothenberg, I. Popov, R. Costi, U. Banin, *Science* **2004**, *304*, 1787.
[18] T. Hirakawa, P. V. Kamat, *J. Am. Chem. Soc.* **2005**, *127*, 3928.
[19] A. V. Akimov, A. Mukherjee, C. L. Yu, D. E. Chang, A. S. Zibrov, P. R. Hemmer, H. Park, M. D. Lukin, *Nature* **2007**, *450*, 402.
[20] H. W. Gu, Z. M. Yang, J. H. Gao, C. K. Chang, B. Xu, *J. Am. Chem. Soc.* **2005**, *127*, 34.
[21] T. Mokari, C. G. Sztrum, A. Salant, E. Rabani, U. Banin, *Nat. Mater.* **2005**, *4*, 855.
[22] P. D. Cozzoli, T. Pellegrino, L. Manna, *Chem. Soc. Rev.* **2006**, *35*, 1195.
[23] J. Yang, H. I. Elim, Q. B. Zhang, J. Y. Lee, W. Ji, *J. Am. Chem. Soc.* **2006**, *128*, 11921.
[24] Y. Khalavka, C. Sönnichsen, *Adv. Mater.* **2008**, *20*, 588.
[25] S. E. Habas, P. D. Yang, T. Mokari, *J. Am. Chem. Soc.* **2008**, *130*, 3294.
[26] C. Pacholski, A. Kornowski, H. Weller, *Angew. Chem.* **2004**, *116*, 4878; *Angew. Chem. Int. Ed.* **2004**, *43*, 4774.
[27] T. Mokari, A. Aharoni, I. Popov, U. Banin, *Angew. Chem.* **2006**, *118*, 8169; *Angew. Chem. Int. Ed.* **2006**, *45*, 8001.
[28] J. Li, H. C. Zeng, *Angew. Chem.* **2005**, *117*, 4416; *Angew. Chem. Int. Ed.* **2005**, *44*, 4342.
[29] H. Yu, M. Chen, P. M. Rice, S. X. Wang, R. L. White, S. H. Sun, *Nano Lett.* **2005**, *5*, 379.
[30] W. L. Shi, Y. Sahoo, H. Zeng, Y. Ding, M. T. Swihart, P. N. Prasad, *Adv. Mater.* **2006**, *18*, 1889.
[31] M. Z. Liu, P. Guyot-Sionnest, *J. Mater. Chem.* **2006**, *16*, 3942.
[32] W. L. Shi, H. Zeng, Y. Sahoo, T. Y. Ohulchanskyy, Y. Ding, Z. L. Wang, M. Swihart, P. N. Prasad, *Nano Lett.* **2006**, *6*, 875.
[33] E. V. Shevchenko, M. I. Bodnarchuk, M. V. Kovalenko, D. V. Talapin, R. K. Smith, S. Aloni, W. Heiss, A. P. Alivisatos, *Adv. Mater.* **2008**, *20*, 4323.
[34] Y. H. Wei, R. Klajn, A. O. Pinchuk, B. A. Grzybowski, *Small* **2008**, *4*, 1635.
[35] B. Nikoobakht, M. A. El-Sayed, *Langmuir* **2001**, *17*, 6368.
[36] L. Dloczik, R. Könenkamp, *Nano Lett.* **2003**, *3*, 651.
[37] D. H. Son, S. M. Hughes, Y. D. Yin, A. P. Alivisatos, *Science* **2004**, *306*, 1009.
[38] R. D. Robinson, B. Sadtler, D. O. Demchenko, C. K. Erdonmez, L.-W. Wang, A. P. Alivisatos, *Science* **2007**, *317*, 355.
[39] J. J. Mock, D. R. Smith, S. Schultz, *Nano Lett.* **2003**, *3*, 485.
[40] A. D. McFarland, R. P. Van Duyne, *Nano Lett.* **2003**, *3*, 1057.
[41] C.-K. Tsung, X. S. Kou, Q. H. Shi, J. P. Zhang, M. H. Yeung, J. F. Wang, G. D. Stucky, *J. Am. Chem. Soc.* **2006**, *128*, 5352.
[42] W. H. Ni, X. S. Kou, Z. Yang, J. F. Wang, *ACS Nano* **2008**, *2*, 677.
[43] T. K. Sau, C. J. Murphy, *J. Am. Chem. Soc.* **2004**, *126*, 8648.
[44] H. J. Chen, X. S. Kou, Z. Yang, W. H. Ni, J. F. Wang, *Langmuir* **2008**, *24*, 5233.
[45] T. Ming, X. S. Kou, H. J. Chen, T. Wang, H.-L. Tam, K.-W. Cheah, J.-Y. Chen, J. F. Wang, *Angew. Chem.* **2008**, *120*, 9831; *Angew. Chem. Int. Ed.* **2008**, *47*, 9685.
[46] V. V. Savant, J. Gopalakrishnan, C. C. Patel, *Inorg. Chem.* **1970**, *9*, 748.

